4

NASA CR-144499
E7.6-10.0.81

Calspan

Technical Report

[redacted]

(E76-10081) S190-INTERPRETATION TECHNIQUES DEVELOPMENT AND APPLICATION TO NEW YORK STATE WATER RESOURCES Final Report (Calspan Corp., Buffalo, N.Y.) 50 p HC $4.00 CSCL 08H G3/43

N76-14564

Unclas
00081

Calspan Corporation
Buffalo, New York 14221

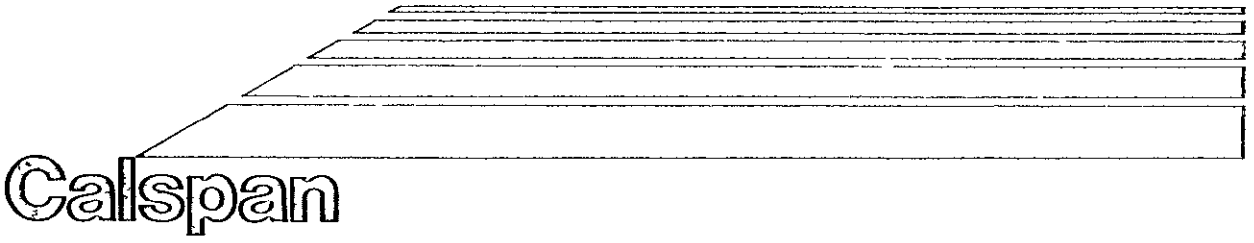

S190 INTERPRETATION TECHNIQUES DEVELOPMENT AND APPLICATION TO NEW YORK STATE WATER RESOURCES

Kenneth R. Piech
John R. Schott
Kenton M Stewart+

Calspan Corporation Report No. YB-5298-M-2

FINAL REPORT

CONTRACT NO. NAS9-13336
EREP NO. 391

JUNE 1975

Prepared for
NATIONAL AERONAUTICS AND SPACE ADMINISTRATION
JOHNSON SPACECRAFT CENTER
HOUSTON, TEXAS 77058

+Department of Biology, State University of New York at Buffalo

Calspan Corporation
Buffalo, New York 14221

ABSTRACT

Correlations between the relative values of the blue and green reflectances of a lake and key water quality indices, such as photic zone depth, Secchi disk transparency, attenuation coefficient and chlorophyll concentration, have been observed during an intensive satellite, aircraft and surface vessel study of Lake Ontario and Conesus Lake. Determinations of relative values of blue and green lake reflectances from Skylab S190A color imagery are in excellent agreement with values obtained from small scale color imagery from aircraft, and the accuracy of the satellite data is within that required for extrapolation to the key water quality indices.

The study has also determined that changes in chlorophyll, lignin and humic acid concentration can be discriminated by the behavior of the blue to green reflectance ratio and the reflectances of the green and red bands. The blue to green reflectance ratio is inversely proportional to chlorophyll concentration, does not vary with humic acid, and is directly proportional to the amount of lignin. The green and red reflectances are directly proportional to both chlorophyll and lignin, while the green reflectance is inversely proportional to humic acid, and the red reflectance is unchanged by humic acid.

The success of the experiment was intimately related to the resolution of the S190 system. The resolution permitted removal of atmospheric effects, which account for approximately two-thirds of the radiance at the spacecraft. Improvements in resolution would permit more accurate data processing, in that atmospheric variations occurring within a large lake could be taken into account in the data processing. In the absence of such improved resolution, the program has developed a method to utilize data from infrared spectral imagery to detect atmospheric variations and account for the effects of the variations in the data processing of the key visible spectral regions which are related to the eutrophication indices.

TABLE OF CONTENTS

LIST OF FIGURES

LIST OF TABLES

Section 1

INTRODUCTION AND SUMMARY

Under the Federal Water Pollution Control Act, the states are required to prepare an identification and classification characterizing the eutrophic conditions of all publicly-owned fresh water lakes within their borders. The scale of such an undertaking renders conventional ground survey techniques unwieldy; for example, a detailed data gathering effort on Lake Ontario alone, or on a system of lakes such as the Finger Lakes of New York State, can require several weeks of investigations.

A single satellite photograph (such as that of Lake Ontario in Figure 1.1) covers an area which would normally take many days to sample using ground techniques. The ability to convert the patterns and tonal variations within such a satellite image to parameters of value to the limnologist would therefore represent a significant advance in the technology of water quality management. The present S190 experiment has investigated the potential of satellite techniques for monitoring the eutrophication indices of such large bodies of water and has demonstrated the feasibility of monitoring eutrophic conditions using satellite techniques.

The geographical area of our study includes Lake Ontario and several inland New York State lakes, specifically Conesus, Chautauqua, Honeoye, and Canadice Lakes. During the Skylab missions, measurements of chlorophyll concentration and optical data were performed from surface vessels on Conesus Lake. Aircraft imagery were obtained of all the above lakes. Our data base also includes several years of physical, chemical and biological data on Conesus, Honeoye and Canadice Lakes, as well as an extensive set of optical data of Lake Ontario obtained from surface vessels and aircraft imagery during the International Field Year of the Great Lakes (IFYGL).[1]

The study of Lake Ontario during 1972 established the feasibility of monitoring selected eutrophication indices using aircraft imagery at scales

FIGURE 1.1. SKYLAB S190A IMAGE OF LAKE ONTARIO, 9 SEPTEMBER 1973. TWO FRAMES OF IMAGERY COVERED THE LAKE ON THIS SKYLAB PASS. THE LARGE URBAN COMPLEX ON THE NORTH SHORE IS TORONTO. THE GREEN DISCHARGE ON THE SOUTH SHORE JUST WEST OF THE NIAGARA RIVER IS THE WELLAND CANAL. RESOLUTION ON THE ORIGINAL TRANSPARENCY IS SUPERIOR TO THAT OF THIS PAPER COPY. FOR EXAMPLE, RUNWAYS AT THE TORONTO AND NIAGARA FALLS AIRPORTS ARE WELL DEFINED ON THE ORIGINAL TRANSPARENCY, AS ARE INDUSTRIAL STORAGE PILES IN THE TORONTO HARBOR. THE NIAGARA FALLS AND THE WHITE WATER OF THE LOWER NIAGARA RIVER CAN BE OBSERVED JUST TO THE SOUTH OF THE TWO POWER STATION RESERVOIRS WHICH STRADDLE THE NIAGARA RIVER. THE ALTITUDE FROM WHICH THIS IMAGE WAS TAKEN WAS 270 MILES (435 KILOMETERS).

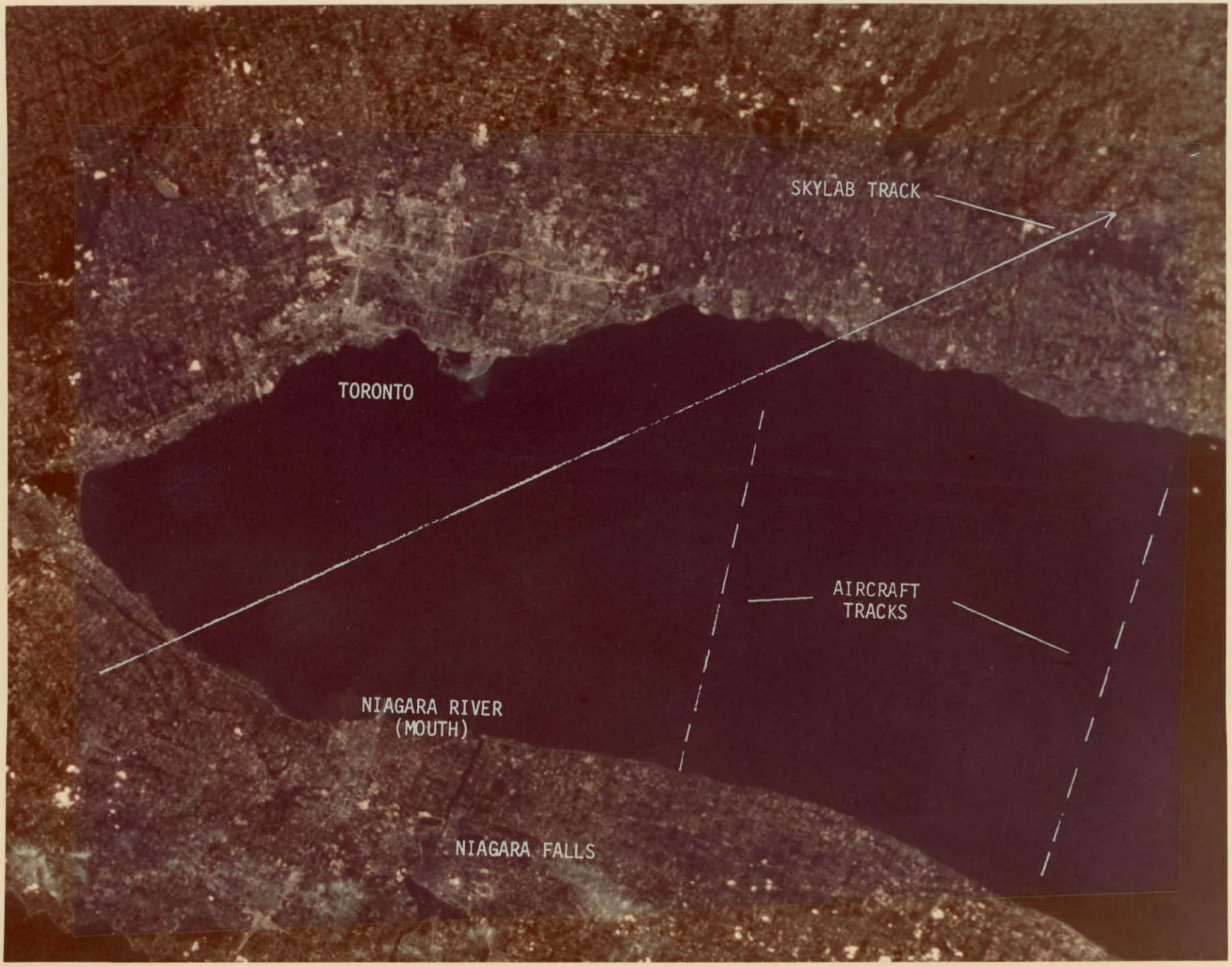

3

as small as 1:50,000. The study demonstrated that indices such as depth of photic zone, Secchi Disk transparency, total attenuation coefficient, and chlorophyll concentration could be related to the relative value of the blue and green reflectances of the lake.* Figure 1.2 exhibits typical correlations found between various parameters on the IFYGL effort. The results of Figure 1.2 are of great importance to the present study and are described more fully in Section 2 below.

Measurement of the relative values of the reflectances is complicated by the low reflectance of the lakes. The exposure in spectral band λ, E_λ, can be approximated by $E_\lambda = \alpha_\lambda R_\lambda + \beta_\lambda$, where R_λ is lake reflectance, β_λ is exposure caused by atmospheric scattering, and α_λ is proportional to atmospheric transmission. At an altitude of 3 km, the proportion of exposure caused by atmospheric scattering to the total exposure to the sensor (β_λ/E_λ) is typically of order 70%. A small change in atmospheric conditions or a small error in measurement of the atmospheric component of exposure thus results in a significant error in lake reflectance. For example, at $\beta_\lambda/E_\lambda = 0.7$, a 10% error in measurement of β_λ causes a 23% error in lake reflectance.

The data analyses are complicated further by spatial variations of the atmosphere over the lakes being studied and by the requirement for accurate repetitive measurements of a seasonal and yearly nature. The aircraft program utilized microdensitometry of shadow targets to measure the flare component of exposure, β_λ,** and microdensitometry of additional scene objects to define the relative illumination and atmospheric transmission within the two spectral bands, $\alpha_{\lambda_1}/\alpha_{\lambda_2}$. The aircraft program was thus able to account for atmospheric variations and measure the relative value of the reflectances, $R_{\lambda_1}/R_{\lambda_2}$, to an accuracy of ±10 percent. Such an accuracy proved sufficient to monitor the eutrophication parameters on a regular basis.

---

*The terms blue, green and red are defined by the spectral sensitivity, or bandpass, of the layers of the color film.

**U.S. Patent 3,849,006.

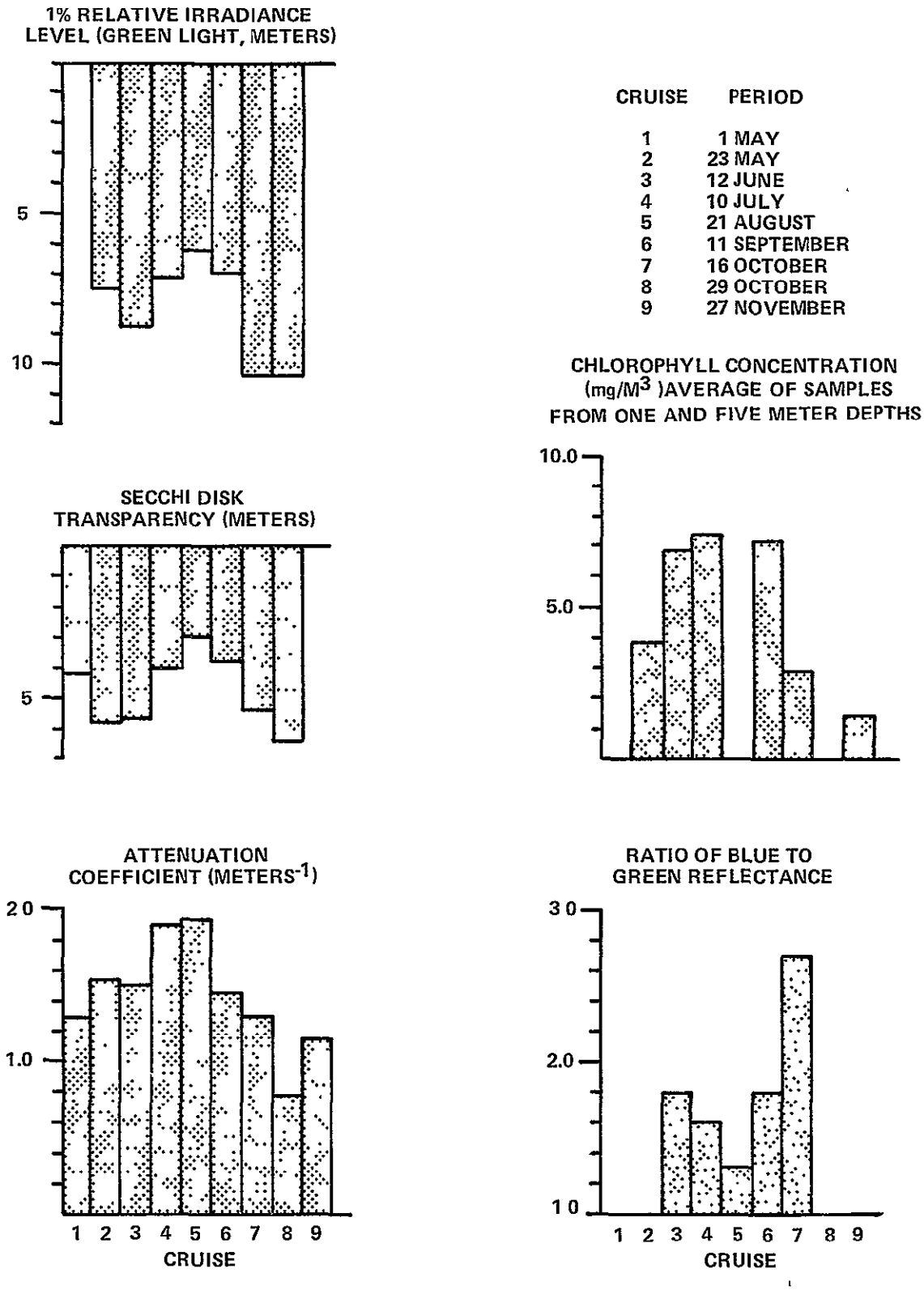

Figure 1.2 COMPARISON OF OPTICAL AND BIOLOGICAL DATA OBTAINED FROM SURFACE VESSEL AND AIRCRAFT MEASUREMENTS DURING THE INTERNATIONAL FIELD YEAR ON THE GREAT LAKES (1972). DATA REPRESENT LAKE-WIDE AVERAGES. CHLOROPHYLL DATA SUPPLIED BY CANADA CENTRE FOR INLAND WATERS.

The resolution of the Skylab imagery is unfortunately not sufficient for image calibration using microdensitometry of shadow targets. In addition, the relation between the eutrophication parameters and the reflectance ratios has been studied only for Lake Ontario. The two key elements necessary for establishing the feasibility of satellite monitoring therefore involve (1) assessment of the photometric accuracy of the satellite imagery, and (2) determination of the universality of the relation between eutrophication indices and lake reflectances. The present investigation has developed and demonstrated a technique to reduce data from Skylab imagery so that the relative values of the lake reflectances can be measured to the required accuracy, in spite of the smaller scale, poorer resolution, and greater atmospheric path of the Skylab imagery. It is apparent from some papers and extensive reviews[2-7] that optical properties of lakes and related chlorophyll values are important in trophic assessments of lakes. Our investigation, involving remote sensing and field work, extends the relationship by comparing both selected eutrophication indices and reflectance ratios for lakes of varying trophic character. Further, a methodology for monitoring changes in chlorophyll, lignin and humic acid concentrations was developed.

The data analysis technique for removal of atmospheric effects utilizes a set of targets of known reflectance to establish values for the unknown parameters α_λ and β_λ. The number of such targets is usually limited to a single locale and the values of α_λ and β_λ are only valid for a region near the known targets because of spatial fluctuations of the atmosphere. The experiment has demonstrated that the change in atmospheric flare exposure, $\Delta\beta_\lambda/\beta_\lambda$, is to good approximation independent of spectral band for a given set of meteorological conditions, and that the ratio $\alpha_{\lambda_1}/\alpha_{\lambda_2}$ is similarly constant. Since the reflectance of the lakes under consideration is effectively zero in the infrared spectral region, measurement of exposure in the infrared spectral band defines $\Delta\beta_\lambda/\beta_\lambda$ and, hence, β_λ at any point over the lake. The necessary information to obtain the reflectance ratio is therefore complete.

The technique was applied to Skylab imagery of Lake Ontario with simultaneous aircraft underflight of two 50 km north-south tracks separated by approximately 50 km. The S190A image of Lake Ontario (Figure 1.1) was processed as discussed above to yield a color encoded display of the blue to green reflectance ratio (Figure 1.3), and the data from this display were compared to aircraft data obtained at an altitude of 3 km and a scale of 1:40,000. About fifteen photographs were obtained on each aircraft track, with each photograph covering an area of about 6.6 square km.[8]

Figure 1.4 depicts the satellite and aircraft data obtained on the two tracks. The aircraft points include error bars corresponding to ±12% of the blue to green reflectance ratio, and ±1.6 km in aircraft position. The correlation between the data is excellent, and the figure indicates that the S190A color imagery is more than adequate for defining the optical properties of the Lake using relationships similar to those obtained on the IFYGL program. Examples of ERTS imagery are also presented within this report in which patterns within Lake Ontario apparently caused by the lake are actually caused by spatial fluctuations of the atmosphere. When atmospheric effects are properly accounted for, the lake patterns are significantly modified.

The relationship between eutrophication parameters and reflectance ratios was studied for Conesus Lake, a small recreational lake within New York State, and a laboratory medium with varying amounts of chlorophyll, lignin, and humic acid. The data reveal that changes in any of these three components can be discriminated by the blue to green reflectance ratio and reflectances of the green and red bands.[+] The blue to green ratio is inversely proportional to chlorophyll concentration, does not vary with the amount of humic acid, and is directly proportional to the amount of lignin. The green and red reflectances are directly proportional to both chlorophyll and lignin, while the green reflectance is inversely proportional to humic acid, and the red reflectance is unchanged by humic acid. All variations are linear over

[+] cf. Table 2.1.

FIGURE 1.3. COLOR ENCODED DISPLAY OF THE RATIO OF BLUE TO GREEN LAKE REFLECTANCE. THE DARK AREA IN THE MIDDLE OF THE IMAGE IS FILM AREA BETWEEN FRAMES OF THE ORIGINAL IMAGERY; THE DARK AREA ON THE RIGHT HAND SIDE OF THE IMAGE IS CAUSED BY A CLOUD BANK WHICH WAS REMOVED IN DATA PROCESSING. THE COLOR CODE IS:

Color	Blue to Green Ratio
Blue	1.2
Red	1.4
Violet	1.5
Pink	1.8
Orange	2.0
Green	2.4
Light Blue	3.1
Yellow	4.2

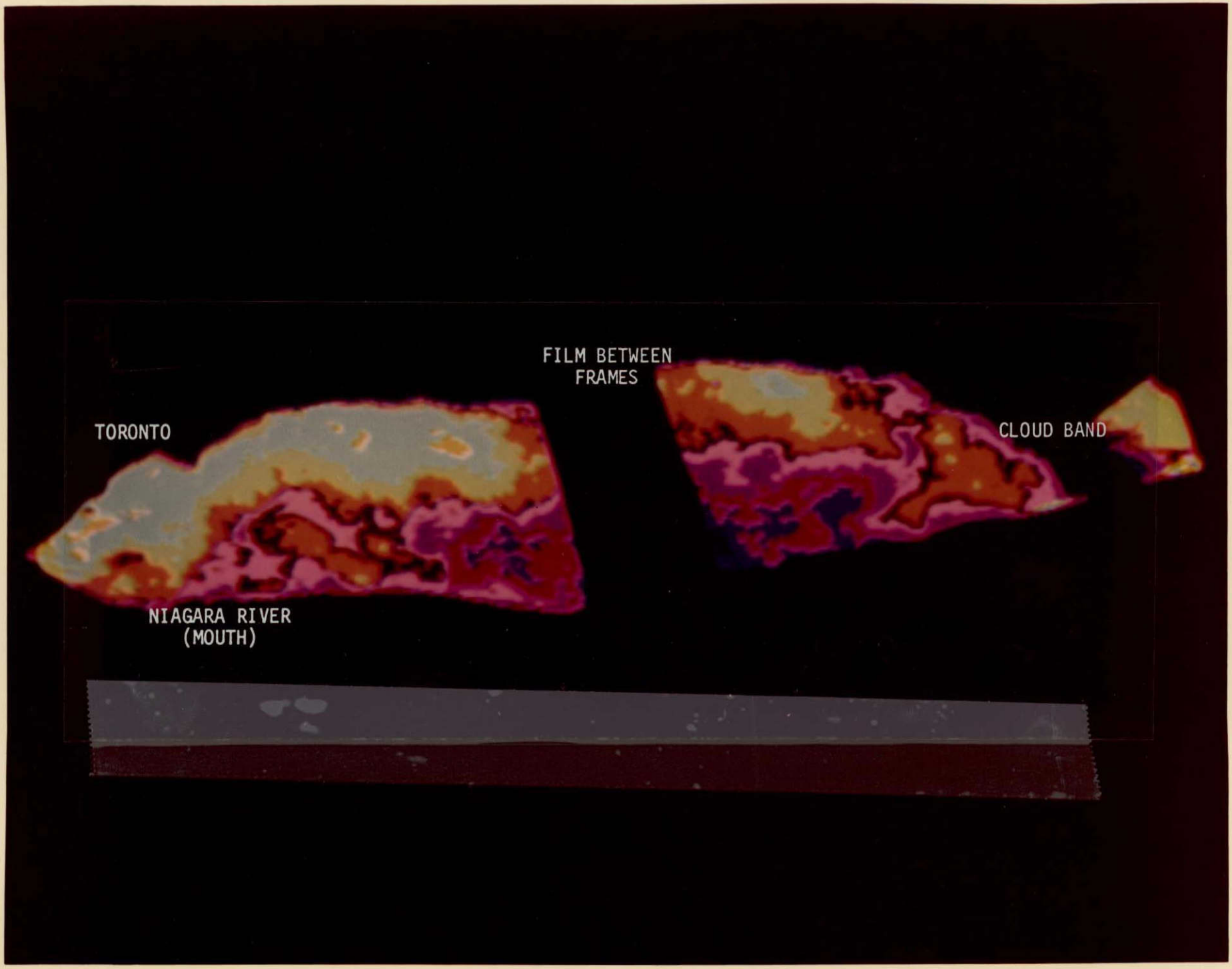


Callaman
AUDIO/VISUAL
PHOTOGRAPHY
79904
Store No.

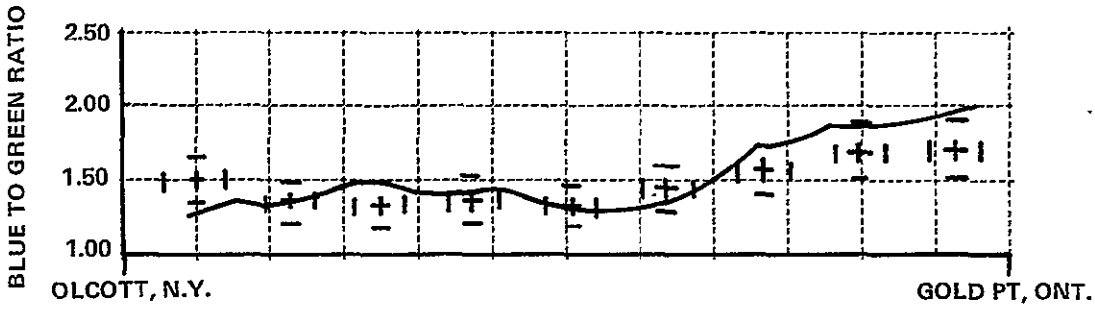

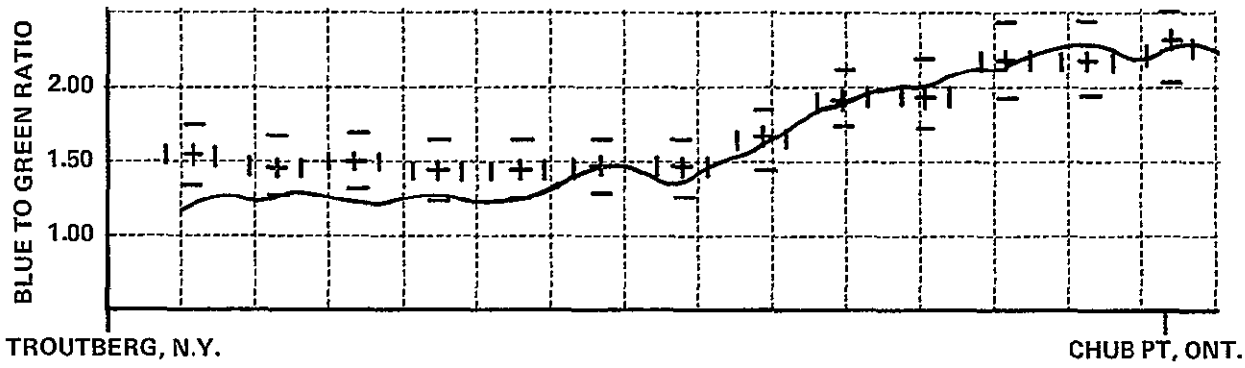

Figure 1.4 COMPARISON OF S190A MEASUREMENTS OF BLUE TO GREEN REFLECTANCE RATIO (SOLID LINE) WITH AIRCRAFT MEASUREMENTS (CROSSES AND ERROR BARS). EACH DIVISION ON THE HORIZONTAL AXIS REPRESENTS 3 MILES, OR 4.8 KILOMETERS.

the range of concentrations observed in practice. Measurements of the blue to green reflectance ratio and green and red band reflectances are thus sufficient to specify variations in chlorophyll, lignin, and humic acid concentration. Application of this methodology to the Skylab image of Lake Ontario in Figure 1.1 indicates that the major variations over the lake are a function of varying chlorophyll concentration.

There are four areas for refinement of the S190 data which we would regard to be of primary importance. An increase in spatial resolution would permit more accurate data processing. Improvement from the present 30 meter range to a resolution of about 5 meters, if possible, would have significant impact on the accuracy of the data processing. Secondly, a systematic overflight program, similar to the repetitive coverage of the ERTS/LANDSAT satellite, would add immeasurably to the value of the satellite data for limnological studies which depend so heavily on temporal comparisons. Thirdly, our knowledge of the relation between eutrophication indices and reflectances of lakes should be improved and extended to a broader range of lake types. Finally, an improved atmospheric propagation model, describing flare exposure changes occurring in different spectral bands, would be of great utility in the study of large lakes where spatial fluctuations of the atmosphere can be of significance.

Subsequent sections of this report discuss the relations between reflectance data and lake parameters, the data processing techniques required for aerial measurement of eutrophication indices, application of data processing to satellite imagery, and study conclusions and recommendations.

Section 2

RELATIONSHIP BETWEEN PHOTOGRAPHIC DATA AND LAKE PARAMETERS

The basis for our comparisons lies in a program conducted during the International Field Year on the Great Lakes (IFYGL). During 1972 the IFYGL program engaged in an intensive study of the physical, chemical, and biological properties of Lake Ontario. As part of the IFYGL effort, the optical properties of Lake Ontario were investigated on nine, week-long cruises at monthly intervals, during which the following optical measurements were made: Sechhi disk transparency, total attenuation coefficient, and sub-surface relative irradiance in red, green and blue spectral regions. In addition to the optical measurements made from the surface vessels, small scale (1:40,000) color aerial photography was obtained concurrent with the surface measurements.

The goals of the optical study were to (1) determine the correlations between the various surface optical techniques; (2) determine the extent of any correlation between optical data obtained from ship and aircraft measurements; and (3) provide input data on temporal and spatial lake fluctuations to other IFYGL programs.

The IFYGL data analyses exhibit important relationships between the surface optical data, surface chlorophyll concentration, and the ratio of blue lake reflectance to green lake reflectance as measured from the color film imagery. Figure 1.2 depicts the variations of blue to green lake reflectance, chlorophyll concentration, attenuation coefficient, photic zone depth (in green spectral region) and Secchi disk transparency. The values depicted are lake-wide averages, i.e., averages over all lake stations occupied.

The data of Figure 1.2 indicate a surprising seasonal relationship between the various parameters. The ratio of blue to green lake reflectance is inversely proportional to chlorophyll concentration and coefficient of total attenuation and directly proportional to photic zone depth and Secchi

disk transparency. Station-by-station comparisons of these parameters are more complex, and a discussion of these data will appear in the IFYGL report; however, the data of Figure 1.2 serve to indicate the general quality and character of the relationships involved.

The specific relationship between the various parameters is dependent on physical properties of the lake being studied. For example, Figure 2.1 contains the relationship between blue to green reflectance ratio and chlorophyll concentration for Conesus Lake, as obtained on the Skylab effort. Again, a strong dependency is evidenced with a marked blue-green minimum occurring at maximum chlorophyll concentration, although the specific relationship of chlorophyll concentration and ratio level differs from the Ontario values. The variation occurs because Conesus and Ontario are quite different in physical character. For example, Conesus is darker than Ontario, having a green reflectance of about 2% compared to a reflectance of 3% for Lake Ontario. The darker the lake, the greater the effect chlorophyll absorption can be expected to have on the blue-green ratio. The actual situation is, of course, more complicated than this simple model.

A major area of further research therefore involves generalizing the relationships between aerial and surface data. By way of example, Conesus and Canadice Lakes have approximately the same range of chlorophyll values and Secchi disk transparencies. The Canadice blue to green ratio values which correspond to the Conesus values of Figure 2.1 are: 7 May, 1.5; 19 June, 0.3; 13 August, no data; and 9 September, 1.4. The close correspondence between the blue-green ratios of Conesus and Canadice, even though specific chlorophyll data for Canadice are not available on these dates, is encouraging. This correspondence, coupled with the correlation of the aerial and surface data for both Conesus Lake and Lake Ontario, leads us to believe that general relationships valid for lakes of a given trophic classification can be developed, and that such understanding will serve to significantly broaden the scope of application of sophisticated satellite photography.

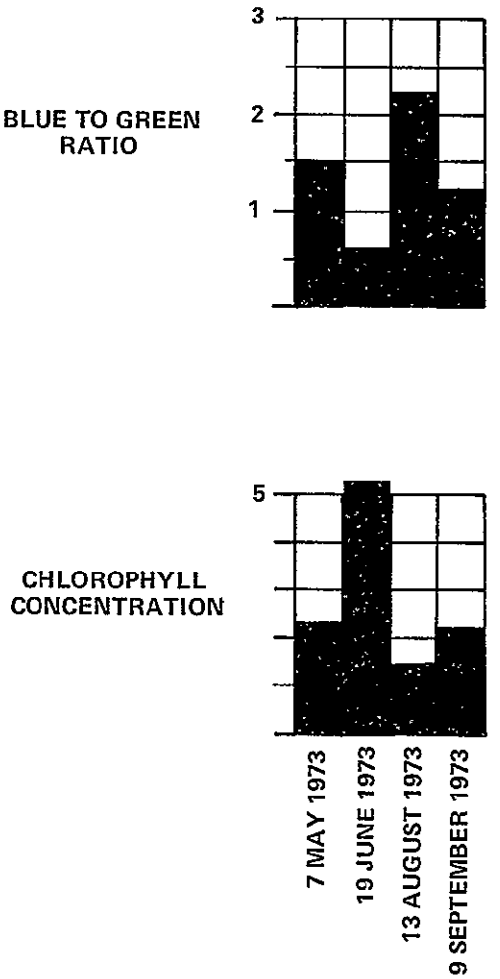

Figure 2.1 COMPARISON OF BLUE TO GREEN REFLECTANCE RATIO WITH SURFACE CHLOROPHYLL CONCENTRATION IN mg/M^3 FOR CONESUS LAKE DURING 1973

A detailed investigation of the relationship between selected eutrophication parameters and reflectance data using imagery and ground survey data of a wide variety of lakes was well beyond the resources of the program. A laboratory experiment was therefore devised to investigate the relationship.

The major difficulties associated with such a laboratory experiment are reproducing the geometry and illumination conditions satisfactorily. The geometry of the problem is that of an infinite half space.* Constructing an approximation to the half space while retaining the ability to vary the parameters of the medium is difficult. Similarly, it is difficult to create satisfactory illumination over the half space approximation.

The above difficulties were resolved by the apparatus of Figure 2.2. A square tube, 0.07 meters on side and 0.5 meters long, was lined with aluminum foil so that specular reflections from the foil would approximate a slab with infinite extent in directions perpendicular to the long axis of the tube. The tube was immersed in a vat of water, approximately 0.5 m^3 in volume, whose composition could be readily changed. A collimated tungsten source illuminated the tube at one end. The light reflected back from the tube was, in turn, collected by a fibre optics probe with a cosine collector head integrated into the photomultiplier tube and electronics of the microdensitometer of the photointerpretation console described below. Measurements were made in red, green and blue spectral bands using Wratten 90 series filters.

The infinite depth of the half space was obtained from the diffuse reflectance, r, and transmission, t, of the tube or slab by iterative computation of the reflectance, r_2, and transmission, t_2, of slabs with double thickness. The necessary equations are

$$r_2 = r + \frac{t^2 r}{1-r^2}, \tag{2-1}$$

$$t_2 = \frac{t^2}{1-r^2} . \tag{2-2}$$

*An infinite half space approximates a large deep lake, i.e., a medium with x and y extent from $-\infty$ to $+\infty$, and z extent from 0 to $-\infty$.

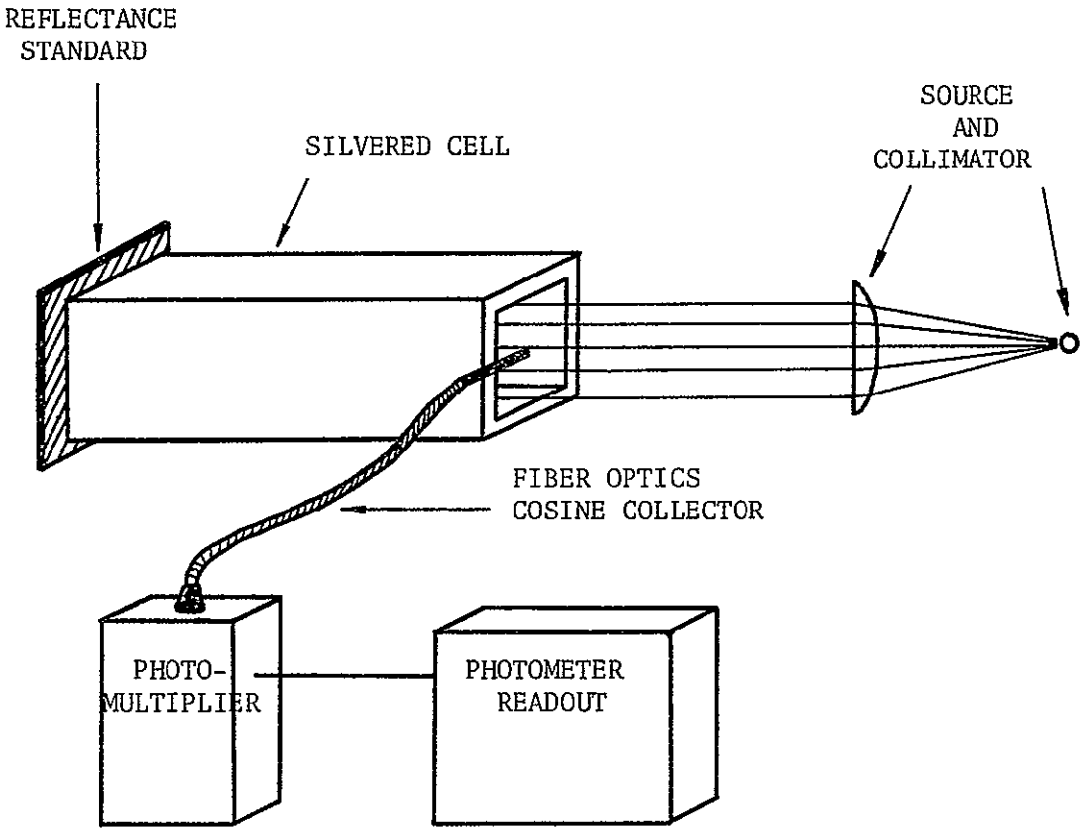

FIGURE 2.2. SCHEMATIC OF LABORATORY APPARATUS FOR REFLECTANCE MEASUREMENT.

The doubling was continued until no change in the reflectance was obtained.

The reflectance and transmission of the medium in the slab, r and t, were measured by monitoring the reflected signal from a set of known reflectance standards at the end of the slab. The reflected signal, S, to first order consists of the signal reflected by the medium alone, s, and that signal transmitted through the medium and reflected by the end reflector, i.e.,

$$S = at^2R + s(r) + c = mR + b \tag{2-3}$$

where R is the reflectance of the end reflector, and a and c are instrument constants. The goodness of fit to the expression Eq. (2-3) for all the test media was always in excess of 0.99. A set of six reflectance standards was used to establish the fit to Eq. (2-3).

The apparatus was calibrated using tap water as a standard. Letting the subscript o denote tap water,

$$S_o = at_o^2R + s(r_o) + c = m_oR + b_o \tag{2-4}$$

The values adopted for tap water transmission in the red, green, and blue spectral bands were 75.0, 93.3, and 98.1% per meter, respectively, or t_o = 86.6%, 96.6%, and 99.0%.

Comparison of the slopes of the test and standard media then yields t through

$$t = t_o\sqrt{\frac{m}{m_o}}. \tag{2-5}$$

The difference between the intercepts of the test and standard media curves yields r through

$$b-b_o = s(r) - s(r_o) \approx s(r), \text{ and} \tag{2-6}$$

$$r = \frac{s(r)t_o^2}{m_o} . \tag{2-7}$$

The properties of the medium were varied by additions of chlorophyll lignin and humic acid. The chlorophyll was added in the form of water-soluble chlorophyll; the lignin was in the form of bleached hardwood paper pulp. Since the chlorophyll was on a soap substrate, the weight of water-soluble chlorophyll necessary to simulate a given concentration of in vivo chlorophyll was determined by matching spectral responses on the standard spectrometer method for measuring chlorophyll concentration. The chlorophyll concentrations were varied from 0 to 7 μg/L, while lignin concentration ranged from 0 to 70 ppm and humic acid from 0.5 to 1.8 ppm.

A major difficulty with the experiment proved to be the soap substrate of the water-soluble chlorophyll. The substrate contributed a white, or approximately spectrally uniform, scattering to the turbidity of the medium. The original intent of the experiment was to modify the chlorophyll concentration while keeping the scattering turbidity as constant as possible. In this way a model could be developed for chlorophyll concentration at varying degrees of background turbidity. Unfortunately, the soap substrate modified the background turbidity as chlorophyll concentration changed. Since this background turbidity was approximately flat spectrally, the net effect was to dampen changes in the reflectance ratios.

Reflectance change with addition of both chlorophyll and lignin was linear. As the amount of chlorophyll was increased, the increased scattering by the substrate effectively cancelled the increasing absorption of the chlorophyll in the blue. The blue reflectance thus remained a uniform 4% from 0 to 7 μg/L. The green reflectance varied from 2.7 to 7.2% over this concentration range, while the red reflectance changed from 1.1 to 2.9%. The corresponding variation in the blue to green reflectance ratio was from 1.5 to 0.6, with the variation being approximately linear. Reflectance of the medium with

lignin variation was 4% to 11% in the blue, 2.7% to 8.5% in green, and 1.1 to 5.7% in red.

The data obtained by individual variation of the three components was supplemented by joint variation of the components. As a result, it was possible to develop a set of discriminators for determining whether a turbidity change is caused by a variation in lignin, chlorophyll or humic acid. The discriminators for the dominant turbidity change are listed in Table 2.1. In essence, the data reveal that changes in any of the three components can be discriminated by the blue to green reflectance ratio and reflectances of the green and red bands. The blue to green ratio is inversely proportional to chlorophyll concentration, does not vary with amount of humic acid, and is directly proportional to the amount of lignin. The green and red reflectances are directly proportional to both chlorophyll and lignin, while the green reflectance is inversely proportional to humic acid and the red reflectance is unchanged by humic acid. Measurements of the blue to green reflectance ratio and green and red band reflectances are thus sufficient to specify variations in chlorophyll, lignin, and humic acid concentration. Use of Table 2.1 in study of the Skylab image of Figure 1.1 indicates that the major turbidity changes are caused by changes in chlorophyll concentration.

Application of the discrimination rules of Table 2.1 would facilitate investigations such as studies of the effects of power plant discharges on neighboring water quality, evaluation of the impact of chlorination of power plant discharges on algal concentration, and a study of the effects of sewage treatment outfalls on stream or river conditions.

By way of example, the discriminators have been applied to simultaneous thermal-IR and color imagery of a portion of the Hudson River between two power plant discharges. Figure 2.3 contains a display of the data generated on both water temperature and eutrophication indices.[+] Data on the eutrophication indices were obtained using the discriminators of Table 2.1 applied to the aerial color imagery.

[+]Thermal image courtesy of New York State Atomic and Space Development Authority.

Table 2.1 DISCRIMINATORS FOR CHANGES IN CHLOROPHYLL, LIGNIN, AND HUMIC ACID

		R	G	B	B/G	G/R	B/R
Chlorophyll	Increase		+/0		-		-
	Decrease		-/0		+		+
Lignin	Increase	+/0	+/0		+/0	-	
	Decrease	-/0	-/0		-/0	+	
Humic Acid	Increase		-		-		-
	Decrease		+		+		+

\+ = increase
\- = decrease
0 = no change

R = red reflectance, etc.
B/G = ratio of blue reflectance to green reflectance, etc.

No entry in a column means the information is not definitive. For a condition to occur, all discriminators must be satisfied; e.g., if the dominant change is an increase in chlorophyll content, both the blue to green and blue to red ratios must decrease, while the green reflectance increases or remains constant.

FIGURE 2.3. APPLICATION OF THE DISCRIMINATION RULES OF TABLE 2.1 TO SIMULTANEOUS THERMAL-IR AND COLOR IMAGERY OF A PORTION OF THE HUDSON RIVER BETWEEN TWO POWER PLANTS.

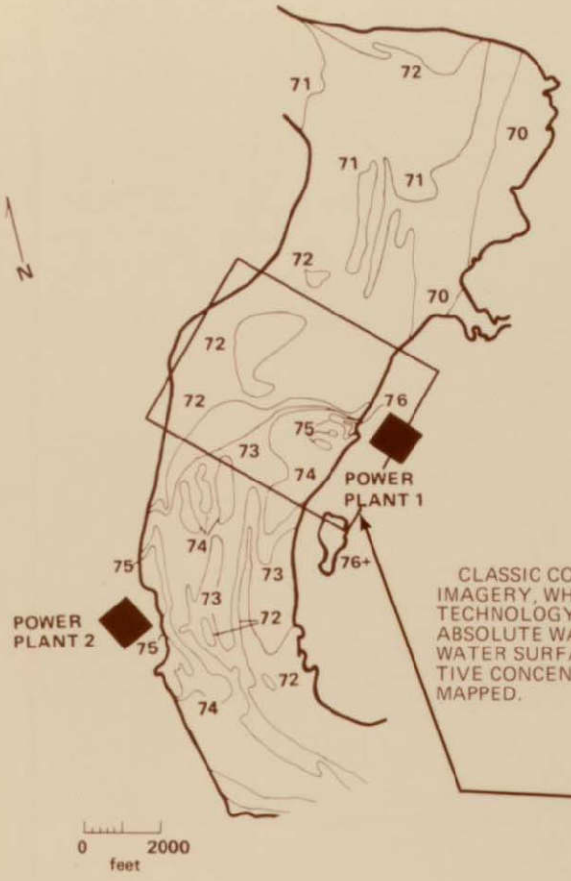

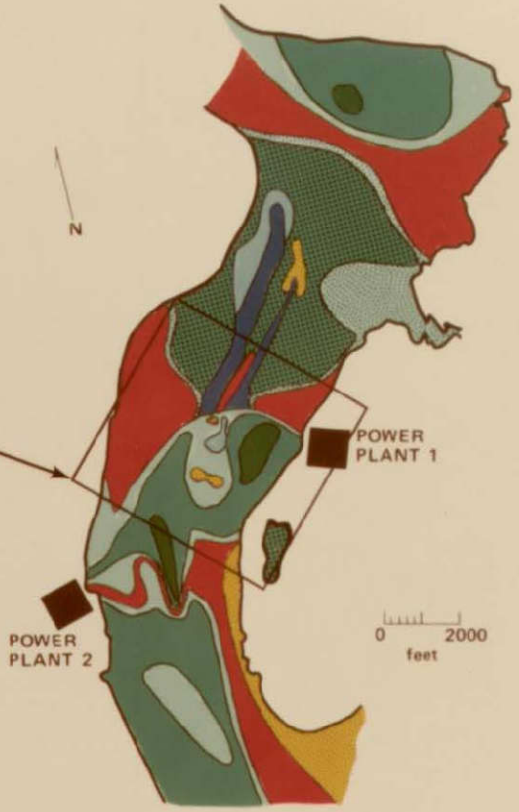

WATER QUALITY BY PATENTED AERIAL SURVEY TECHNIQUES

CLASSIC COLOR AERIAL PHOTOGRAPHY AND THERMAL SCANNER IMAGERY, WHEN CALIBRATED AND ANALYZED BY ADVANCED TECHNOLOGY, RESULTS IN ACCURATE WATER QUALITY MAPPING. ABSOLUTE WATER SURFACE TEMPERATURES TO ±1°F, RELATIVE WATER SURFACE TEMPERATURES TO 0.4°F, ABSOLUTE AND RELATIVE CONCENTRATIONS OF CERTAIN POLLUTANTS CAN ALSO BE MAPPED.

Thermal Image Courtesy of New York State Atomic and Space Development Authority

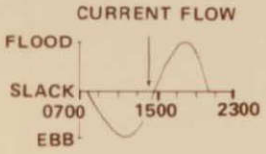

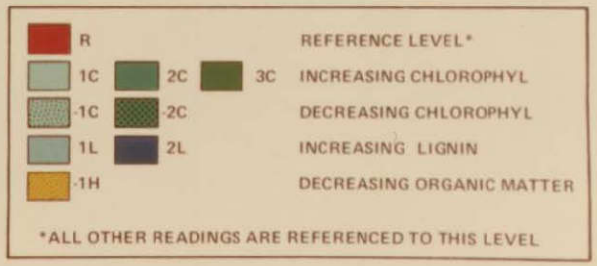

Comparative analysis of data from the thermal and color imagery yields some interesting results on the effects of the two power plant discharges. The chlorophyll concentration increases in the river from Power Plant 1 proceeding south (downstream). The northern boundary of the increase in chlorophyll concentration from the upstream levels corresponds well with the shape and location of the increased water temperature from the two discharges. In the area south of Plant 2, the increased chlorophyll concentration predominates on the western half of the river, which is the area of the river into which the warmer discharge waters are primarily confined (cf. thermal data map). The spring-fed pond just to the south of Plant 1 on the eastern shore appears very blue in the color image, especially when compared to the green of the neighboring river water. This pond has very little algal concentration, which is manifested by the low chlorophyll concentration extracted from the color image. We would expect such comparative analyses of thermal and color imagery to yield increasingly important results as the analysis techniques are applied to a broader spectrum of problems.

Section 3

DATA PROCESSING METHODS

The data reduction removes effects of film processing and atmospheric and illumination variations from the tonal variations of the color film image. Processing effects are easily accounted for through use of D-log E curves. As a result, film density variations can be translated to changes in relative exposure at the spacecraft or aircraft.

The resultant exposures, however, must still be related to reflectance values. Such reduction is important because exposure depends on meteorological conditions, altitude of measurement, and illumination conditions, such as proportion of sunlight to skylight and the amount of air light (the contribution to exposure by illumination scattered to the camera by the air column beneath the camera). These effects are depicted in Figure 3.1.

All of these effects can be approximately coupled into three parameters for a given spectral band: α, α', and β.[9-11] The parameter α is proportional to atmospheric transmittance and total (sunlight + skylight) irradiance; α' is proportional to atmospheric transmittance and skylight irradiance; and β is proportional to the amount of air light in the scene. The exposure, E, in sunlight of an object with reflectance R is

$$E = \alpha R + \beta, \tag{3-1}$$

whereas the exposure of the same object in shadow, E', is

$$E' = \alpha' R + \beta. \tag{3-2}$$

Color film measurement of terrain reflectance thus requires knowledge of α, α', and β in each of the three color film bands.

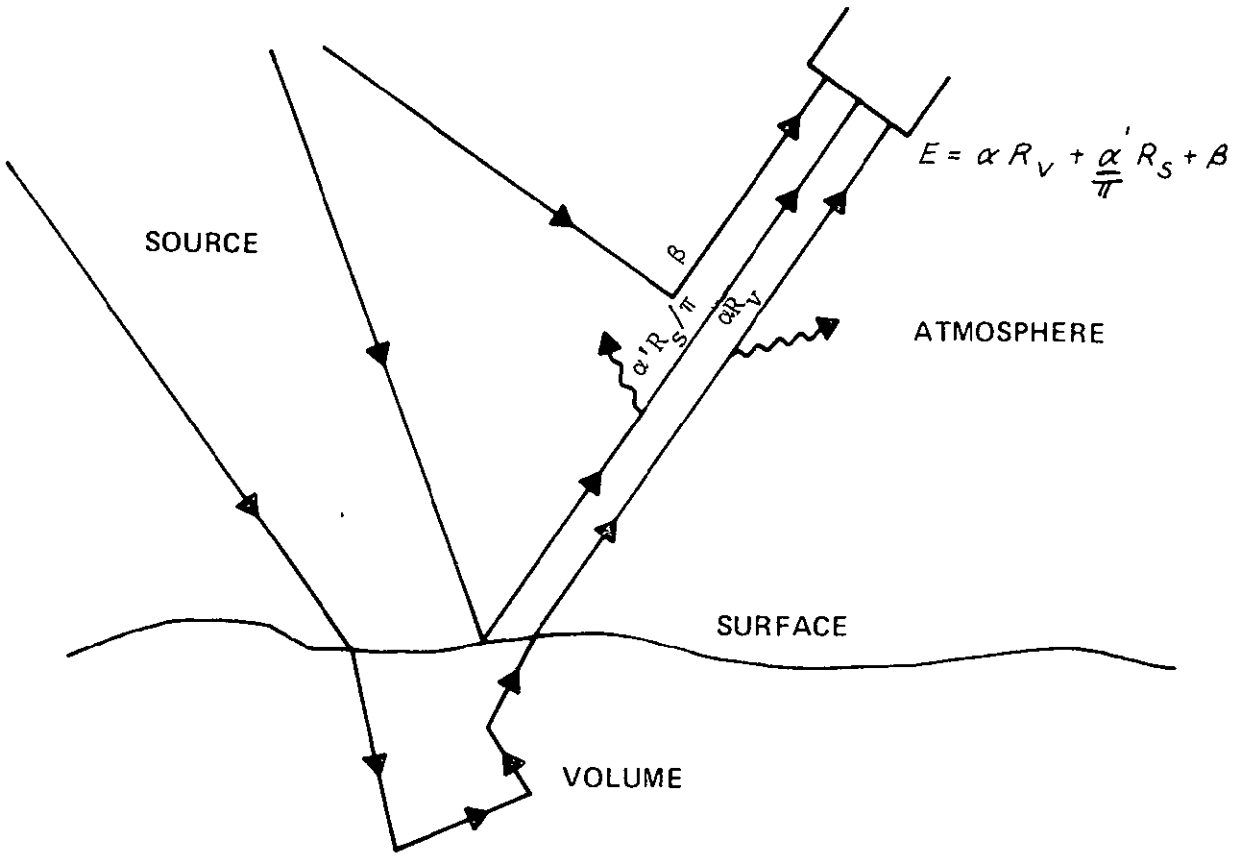

FIGURE 3.1. ATMOSPHERIC AND ILLUMINATION EFFECTS INVOLVED IN ESTABLISHING THE EXPOSURE OF A BODY OF WATER.

The parameter α' is important because it permits removal of specular skylight reflections from the data. Specular surface reflections of skylight exist at every image point of a body of water. Letting R_V be volume reflectance of the body of water and R_S the Fresnel surface reflectance (which is known from metric considerations), the exposure from a body of water can be written

$$E = R_V + \frac{\alpha'}{\pi} R_S + \beta. \qquad (3\text{-}3)$$

Knowledge of α' thus permits subtraction of specular skylight surface reflection.

The (α, α', β) parameters can be determined using a shadow calibration procedure called the Scene Color Standard (SCS) technique*. Calibration is accomplished by densitometry of the illumination discontinuities at shadow edges. In the sunlight just outside a shadow the exposure E is given by Equation (3-1). Just inside the shadow, the exposure E' is given by Equation (3-2). Equations (3-1) and (3-2) yield

$$E = \alpha/\alpha' \; E' + \beta(1-\alpha/\alpha') \qquad (3\text{-}4)$$

Equation (3-4) is a linear relationship between E and E' with slope α/α' and intercept $\beta(1-\alpha/\alpha')$. Two shadows determine the slope and intercept and, hence, β and α/α'. In practice a number of shadows are analyzed, and a least squares fit is made to the data. Figure 3.2 shows typical calibration curves for calibration of a color image at a scale of 1:40,000.

The essential measurement and atmospheric conditons have now been determined. One aspect remains: that of establishing an absolute level of reflectance, akin to laboratory use of a MgO standard or its equivalent. A tar or sheet asphalt scene element in sunlight (roadway, roof) is usually used

*U.S. Patent 3,849,006

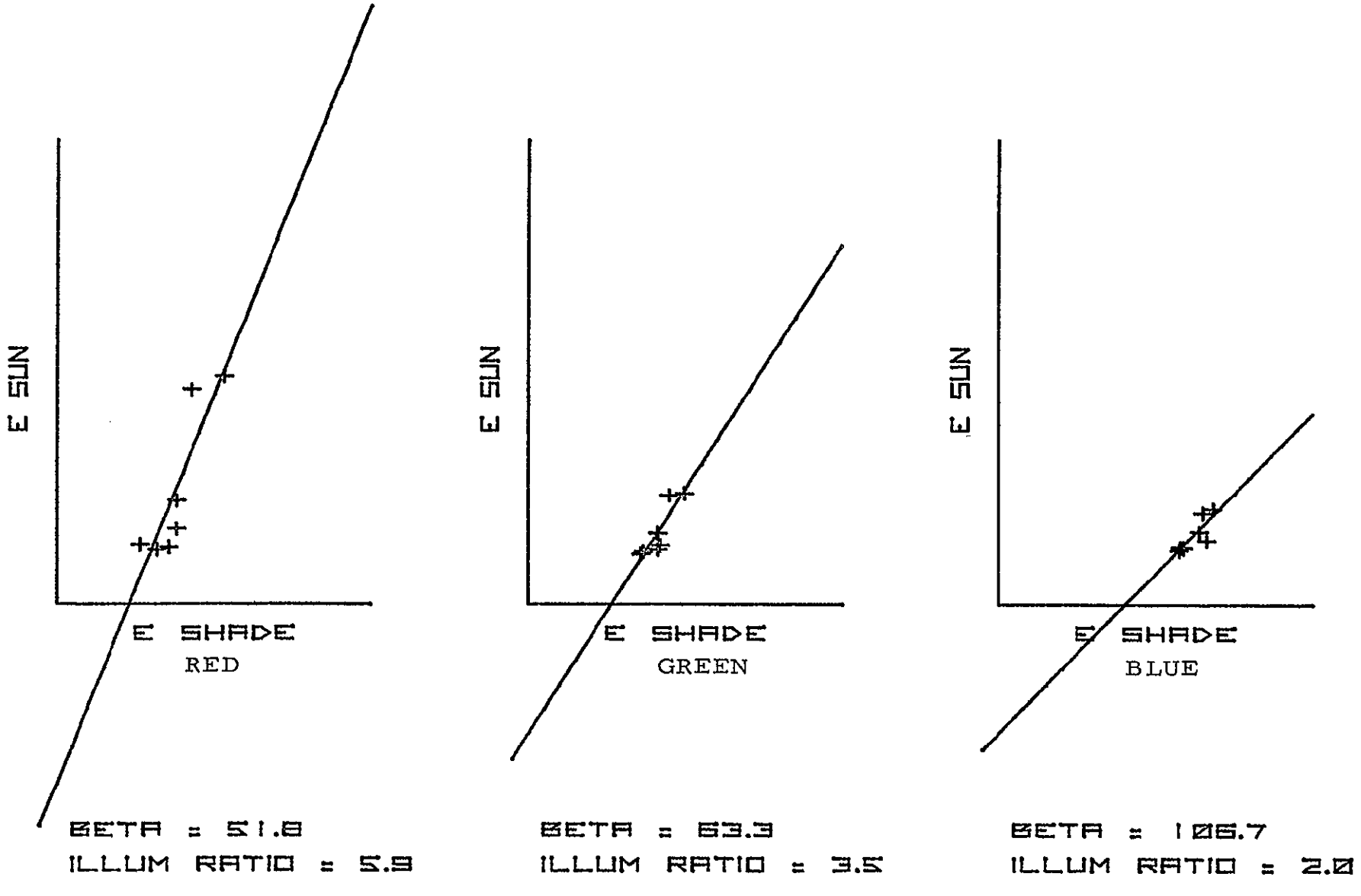

FIGURE 3.2. TYPICAL CALIBRATION CURVES FOR A COLOR IMAGE AT A SCALE OF 1:40,000. THE PARAMETER "ILLUM RATIO" IS $(\frac{\alpha}{\alpha'} - 1)$ (CF. TEXT).

to establish the value of α and complete the calibration. These elements are used as: (1) their reflectances are spectrally flat; (2) their reflectances remain constant over the year; and (3) their reflectance can be easily estimated or measured. Other objects more appropriate for a particular survey can, of course, be used.

Under conditions where only reflectance ratio values are required, it is not necessary to know the reflectance of a scene element. Instead, the exposure values in one spectral band are plotted against the exposures in another band for a range of flat reflectors. The points obtained are then fit to a straight line in an analysis similar to that shown in Figure 3.2 for obtaining beta. The slope of the line thus obtained is equal to the ratio of the alpha values in the two bands. In practice a slight correction is made to this value to account for the fact that most targets generally assumed spectrally flat are not actually uniform reflectors. Using the relative alpha values obtained in this manner, the reflectance ratios can be obtained. Furthermore, if the reflectance of a terrain object in any one band is known, then the absolute alpha value for the band can be obtained as described above. The remaining alpha values can then be obtained from the alpha ratio values.

One minor point needs to be added for completeness. The skylight irradiance inside and outside the shadow is only some portion of the sky dome, k, due to solid angle shielding by the shadowing object. The factor k can be easily determined from metric considerations. In practice at high altitudes only larger buildings suffice for densitometry, and k is practically constant for all the structures utilized. The factor α' in Equations (3-1), (3-2), and (3-4) should therefore be replaced by $k\alpha'$ and interpretation of the resulting values of slope and intercept so modified.

At an altitude of 10,000 feet, β can be equivalent to about a 5-10 percent reflector. At low altitudes, β will usually not decrease much below a 2-3 percent equivalent reflector because of camera flare, which is included in the additive light factor represented by β. It must be emphasized that the actual values of β will depend strongly on meteorological conditions, the

spectral band (bandwidth, central wavelength) in which the measurement is made, and the flare characteristics of the instrument utilized. Because of the wide variation of β (and also α and α') with atmospheric, illumination and measurement system variables, exposures must be carefully reduced to reflectances for meaningful limnological assessments.

A photointerpretation console which enables the interpreter to calibrate color film quickly and accurately has been fabricated for the Reconnaissance Applications Section, Rome Air Development Center, United States Air Force. A similar console is available at Calspan's Buffalo facility. The console also enables the interpreter to obtain color encoded displays of spectral reflectance ratios from the color imagery. Figure 3.3 contains a schematic of the experimental photointerpretation console. The console provides the imager interpreter with all of the capabilities he presently utilizes; i.e., (1) a variable illumination light table and (2) zoom stereo magnification with reticules and scales for mensuration in a convenient location. However, in addition, (3) a micro-macro densitometer capability, (4) a desk calculator and display capability, and (5) a CRT color display capability are provided to facilitate removal of atmospheric effects and present reflectance ratio information to the interpreter. To generate the reflectance ratio information, another light table (6) is required to photographically copy and develop (7,8) the spectral ratio imagery which is then displayed to the density slicing and color encoding vidicon (9) for display on the color CRT, through a control panel (10). Further details of the interpretation console may be found in Ref. 12.

Using the shadow analysis procedure discussed above, the relative value of reflectances in two spectral bands can be measured to an accuracy of about $\pm$12% of the reflectance ratio value. To indicate the general level of accuracy and consistency which can be expected under operational conditions, measurements of the ratio values of a set of unchanging targets made over a one-year time period are presented, as well as measurements of a set of targets from different altitudes on the same day.[13]

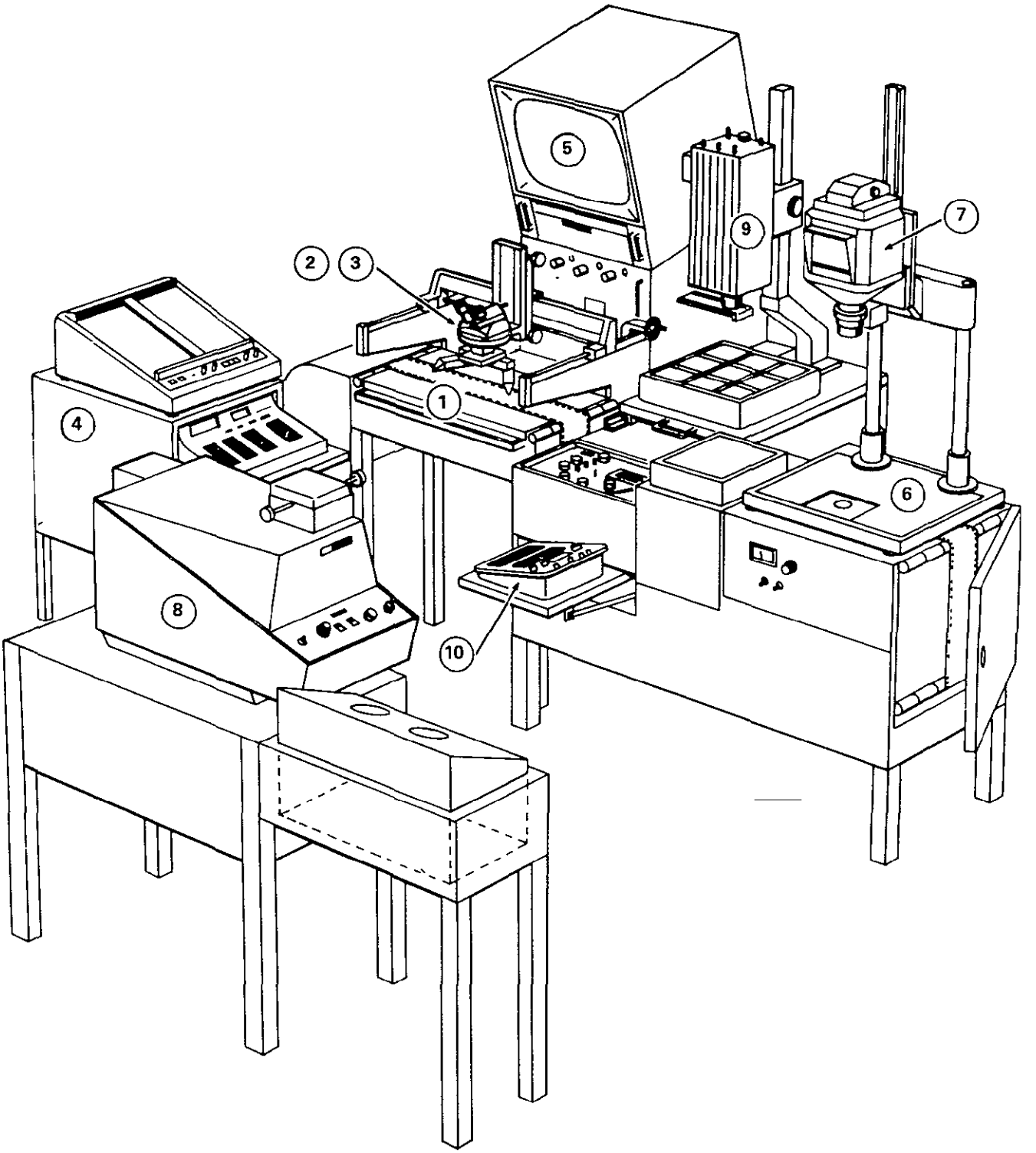

FIGURE 3.3. THE EXPERIMENTAL PHOTOINTERPRETATION CONSOLE. THE CONCEPT AND DEVELOPMENT OF THE CONSOLE WAS SPONSORED BY ROME AIR DEVELOPMENT CENTER, U. S. AIR FORCE.

Table 3.1 contains a listing of nine targets whose reflectances can be expected to remain relatively constant. The targets were overflown under widely differing weather conditions on five occasions between August 1972 and September 1973. Flight altitude was about 10,000 feet (3 km), and scale about 1:40,000. The red to green and blue to green ratio values for these targets and the standard deviation for the aerial measurements are also listed. The average standard deviation, in percent, is 13% for the red to green measurements and 10% for the blue to green values. The accuracy is sufficient to permit monitoring of changes in the selected eutrophication indices described in Figure 1.2 above.

Table 3.1

TEMPORAL VARIATION OF RATIO MEASUREMENTS

	Target	Red to Green	Blue to Green
1.	Light Roof	1.52 ± 0.14	1.06 ± 0.08
2.	Asphalt	1.49 ± 0.20	0.92 ± 0.07
3.	Gravel	1.29 ± 0.16	1.02 ± 0.09
4.	Red Roof	2.71 ± 0.37	0.79 ± 0.14
5.	Dark Roof	1.15 ± 0.17	0.78 ± 0.14
6.	Gray Roof	1.42 ± 0.19	0.95 ± 0.06
7.	Dark Roof	1.09 ± 0.15	1.17 ± 0.08
8.	Black Roof	1.18 ± 0.17	1.10 ± 0.09
9.	Light Gray Roof	1.28 ± 0.18	1.17 ± 0.11

Figure 3.4 contains a comparison of the blue to green reflectance ratios obtained at different altitudes for a set of fifteen objects. The ratio values were obtained from an altitude of 14,500 feet (4.4 km) with scale of 1:29,000 and from an altitude of 4,000 feet (1.2 km) with scale of 1:8,000. The data were obtained on the same day within a closely spaced time

interval. The line of exact correspondence, on which points would lie for the case of perfect data processing, is delineated in the figure. The data points lie in good agreement with this line, indicating proper removal of atmospheric effects. The accuracy of the reflectance ratios at each altitude is ±12% of the measured value. The values of β, in equivalent reflectance, for the 4,000 feet imagery were 1.8, 1.5 and 1.7% in red, green and blue respectively. The values for the 14,500 foot imagery were 3.2, 3.1 and 4.5%. The spectral character of the flare is uniform at the lower altitude. At 14,500 feet the flare has adopted a strong blue character.

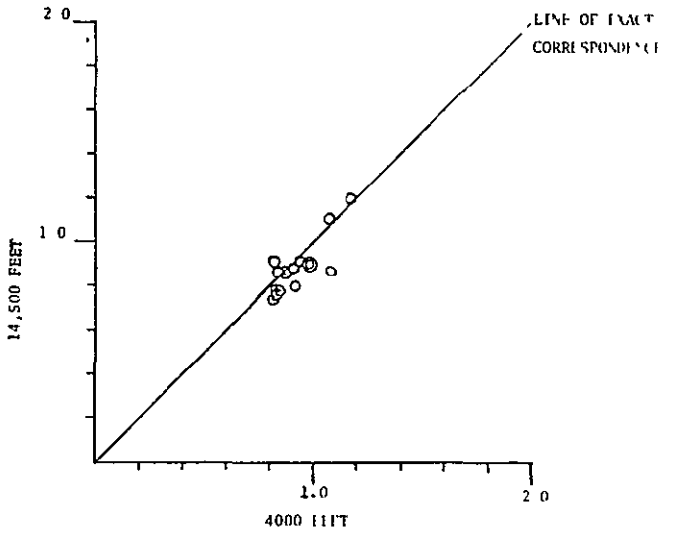

Figure 3.4. CORRELATION BETWEEN BLUE TO GREEN REFLECTANCE RATIOS MEASURED AT 14,500 FEET (SCALE 1:29,000) WITH THOSE MEASURED AT 4,000 FEET (SCALE 1:8,000).

Section 4

SATELLITE DATA PROCESSING

The resolution of the S190 experiment precludes use of the shadow calibration technique described above.[+] In lieu of the shadow technique, large reflectance standards can be used for calibration, as in the Lake Ontario example cited in Section 2. The accuracy provided by the reflectance standard method appears adequate for the eutrophication analyses, although the ultimate solution to the calibration question would be an improvement in S190 resolution so that large shadows could be utilized.

Logistical considerations restrict use of reflectance standards to a small number of locations. Weather variations over an area the size of Lake Ontario can restrict the validity of calibration data obtained from a given location. Until system resolution is improved, a technique for measuring atmospheric changes relative to a given locale would be valuable. The present experiment has found that atmospheric changes can be so measured through use of the infrared reflectance region.

Atmospheric changes manifest themselves in changes in the flare parameter, β, and the illumination-transmission parameter, α. Measurement of reflectance ratios requires knowledge of β in each spectral band and of the ratio of the α values in the two spectral bands.

Analysis of a large data set obtained during the IFYGL effort and the Skylab program indicates that the ratio of α values between any two bands remains constant on a given day. Table 4.1 contains a listing of the average relative α values and percent standard deviation of relative α values for the flights conducted in 1972 and the 1973 Skylab flights. The percent standard

[+]The shadow calibration technique has been successfully applied, on ERTS imagery, to both cloud shadows and shadows generated by large terrain features. Use of such objects is considered a special case.[14]

Table 4.1- VARIATION OF ALPHA RATIOS OVER LAKE ONTARIO

Mission Date	Green to Red Alpha Ratio			Blue to Green Alpha Ratio		
	$\bar{x}$	σ	$\sigma/\bar{x}$(%)	$\bar{x}$	σ	$\sigma/\bar{x}$(%)
16 June 1972	1.50	0.01	1	1.75	0.22	13
27 June 1972	0.62	0.05	7	0.74	0.04	6
17 July 1972	0.59	0.11	18	0.73	0.08	11
30 August 1972	0.57	0.10	17	0.87	0.13	15
11 Sept 1972	0.54	0.05	9	0.72	0.10	15
19 Oct 1972	0.66	0.13	20	0.75	0.06	8
13 August 1973	0.43	0.02	5	0.55	0.06	11
9 Sept 1973	1.01	0.13	13	1.03	0.14	14
	Average $\sigma/\bar{x}$(%):		11			12

$\bar{x}$ = mean

σ = standard deviation

deviation over the entire lake is small, taking into account that the shadow measurement of the relative values of the parameter α has an accuracy of $\pm 10\%$, and that the variations represent atmospheric changes occurring over an area of 50 x 150 miles, or 7,500 square miles.

Similar analysis of the 1972 IFYGL and 1973 Skylab data suggest that the atmospheric flare values between two spectral bands are linearly related. Measurement of flare changes in any one band would therefore define the flare change in any other band. Fortunately, the reflectance in the infrared spectral region (0.7 μ to 1.0 μ) of a lake such as Ontario is effectively zero. The infrared exposure at any format point is due soley to flare exposure, and changes in exposure across the lake can therefore be related to changes in atmospheric flare.

The slopes (m), intercepts (b), and goodness of fit coefficients (r^2) for three IFYGL data missions are listed in Table 4.2. An atmospheric model relating flare exposure in the various spectral bands has not been developed and, as a result, it is not possible to use the relationships of Table 4.2 for predictive purposes. We have found, however, that the flare changes can be described by

$$\frac{\beta_{\lambda_1}(x)}{\beta_{\lambda_1}(x')} = \frac{\beta_{\lambda_2}(x)}{\beta_{\lambda_2}(x')} \quad , \tag{4-1}$$

where x and x' denote different locations. Eq. (4-1) can be easily recognized as an approximate form of the relations of Table 4.2. Thus, until an adequate atmospheric model is developed, flare exposure variations can be determined from measurements in the infrared spectral band and the approximate relation Eq. (4-1). An equivalent form of Eq. (4-1) is that $\Delta\beta_\lambda/\beta_\lambda$ is independent of spectral band.

Table 4.2 PARAMETERS OF THE EXPRESSION

$$\beta_i = m\beta_j + b$$

Mission Date	i = Green, j = Red			i = Blue, j = Green		
	m	b	r^2	m	b	r^2
17 July 1972	1.21	-14.0	0.61	1.17	45.9	0.73
30 August 1972	0.69	17.0	0.59	1.47	7.3	0.77
11 September 1972	0.47	43.3	0.75	0.95	37.7	0.87

No significant atmospheric variations occurred over Lake Ontario in the Skylab image of Figure 1.1. For example, the flare values at the four endpoints of the two widely separated flight tracks varied from 7.2 to 8 units in the blue spectral band, and 4.4 to 5.2 units in the green band.

An example of atmospheric changes creating apparent changes in lake patterns is contained in Figure 4.1, an ERTS image of Lake Ontario. The exposure over the lake in band 6 (0.7 μ - 0.8 μ) should be uniform. Patterns, however, exist within the lake which are quite similar to the patterns of band 4 (0.5 μ - 0.6 μ). Much of the variation observed over Lake Ontario on this pass is therefore due to atmospheric effects, as opposed to lake effects. Note in particular the apparent change in lake properties occurring at arrow A in the green band, which is duplicated at arrow A in the infrared band. Much of this change is due to a variation in atmospheric properties. The green band change occurring at arrow B, however, is not duplicated in the infrared band. Here the change is effected by a physical change in lake properties. A simple evaluation of the infrared band therefore provides a determination whether observed lake patterns are genuine or caused by atmospheric effects.

FIGURE 4.1. ANALYSIS OF AN ERTS IMAGE OF THE EASTERN END OF LAKE ONTARIO. THE UPPER DISPLAY IS A BLACK AND WHITE PRINT OF BAND 4, WHILE THE MIDDLE AND LOWER FIGURES ARE COLOR ENCODED DISPLAYS OF BANDS 6 AND 4, RESPECTIVELY. IF ATMOSPHERIC CONDITIONS WERE CONSTANT OVER THE LAKE, THE BAND 6 DISPLAY WOULD BE UNIFORM.. THE BAND 4 DISPLAY WOULD THEN DEPICT CHANGES IN LAKE CONDITIONS. THIS IS NOT THE CASE, HOWEVER, AS EVIDENCED BY THE CHANGES AT ARROWS A. HERE MUCH OF THE APPARENT CHANGE IN LAKE PROPERTIES IS CAUSED BY AN ATMOSPHERIC FLUCTUATION. THE CHANGE AT ARROW B, ON THE OTHER HAND, IS NOT DUE TO AN ATMOSPHERIC EFFECT.

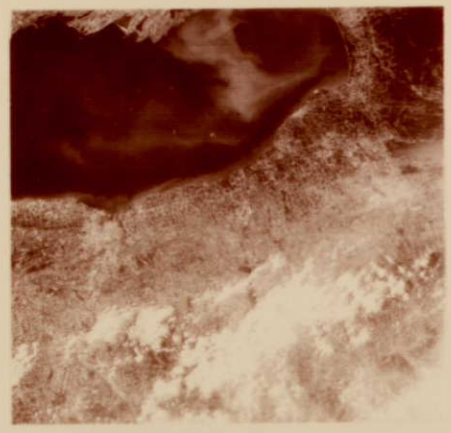

ERTS BAND 4 IMAGE OF THE WESTERN END OF LAKE ONTARIO, 9 JULY 1973.

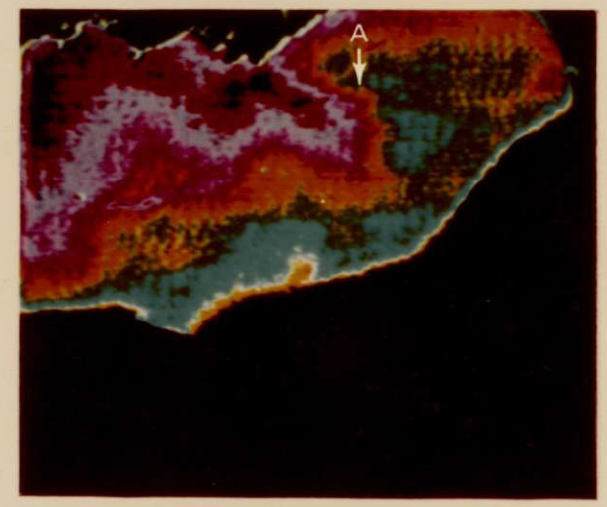

COLOR ENCODED DISPLAY OF AN ENLARGED PORTION OF THE ABOVE FRAME, BAND 6.

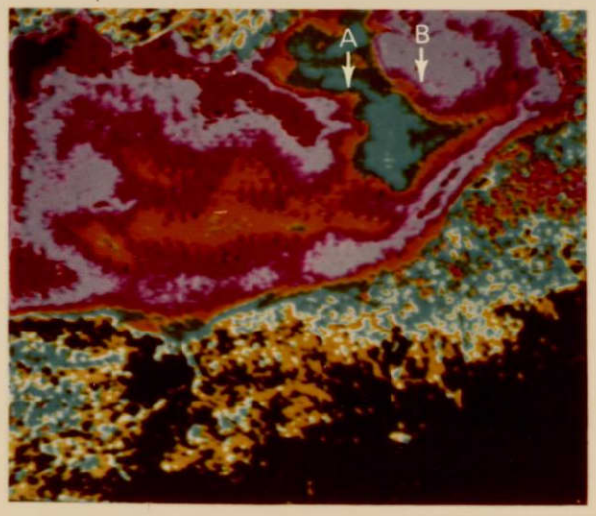

COLOR ENCODED DISPLAY OF AN ENLARGED PORTION OF THE ERTS FRAME, BAND 4.

The techniques which have been applied to the color imagery and to the ERTS data can also be applied to filtered black and white imagery. The filtered black and white Skylab frames were not analyzed in detail because the color imagery was more than adequate for solution of the problem. Data collection and data processing are far more convenient for color imagery, and we would therefore recommend that color imagery be selected over any black and white options in future mission planning.

Section 5

CONCLUSIONS AND RECOMMENDATIONS

Our S190 investigation of Lake Ontario and Conesus Lake has yielded the following results.

(1) The program has demonstrated that Skylab imagery can be utilized to regularly monitor key eutrophication indices of lakes, such as chlorophyll concentration and photic zone depth. The prime characteristic of the imagery necessary for the monitoring is the resolution of the experiment. The resolution permits the data processing necessary to remove atmospheric effects which can account for approximately two-thirds of the signal at the spacecraft.

(2) The program has extended the understanding of the relation between the blue to green reflectance ratio and chlorophyll concentration and has demonstrated that changes in lake properties caused by important parameters, such as chlorophyll, lignin and humic acid, can be discriminated using reflectance ratios and reflectance changes.

(3) The program has developed a data processing technique for detecting atmospheric fluctuations occurring over a large lake and for accounting these fluctuations in an approximate manner in the data processing of the key visible spectral bands.

Our investigation has resulted in the following recommendations concerning satellite monitoring of eutrophication indices.

(1) The primary improvement for satellite monitoring systems would be an increase in resolution. The increased resolution would permit use of a more accurate data processing technique, namely the shadow calibration process used in aircraft eutrophication studies. The shadow calibration is not only more accurate than the calibration by reflectance standards necessitated by the current S190 resolution, but it also can be applied to a larger number

of areas surrounding the lake, thereby improving the data processing. An increase in resolution to about 5 meters, if possible, would permit use of the shadow calibration technique.

(2) Increased effort should be expended in developing an improved model of the relation between lake reflectance and key eutrophication parameters. Our current understanding is such that the reflectance and relative values of the reflectances can be used to detect changes in eutrophication indices and to discriminate variation in lake properties caused by substances such as chlorophyll, lignin and humic acid. The current understanding is semi-empirical, and an improved model valid for lakes of different trophic classification and turbidity level would be a significant advance for satellite monitoring of eutrophication.

(3) Exposures of future lake imagery should be increased by one stop. All available S190 red spectral bands (both color films and filtered black and white) were underexposed to the point where the red information was on the shoulder of the D-log E curve. Lakes are darkest in the red spectral band, being of the order of a 1% reflector in all but regions of unusually high sediment content. Corrections for flare exposure become extremely critical for such a dark target, with a small error in flare measurement causing a large error in the resulting lake data. The underexposure made accurate sensitometry and data processing extremely difficult for the present Skylab experiment.

(4) Future satellite systems must include the feature of regular repetitive coverage. A systematic overflight program, similar to the repetitive coverage of the ERTS/LANDSAT satellite (at intervals of about two weeks), would add immeasurably to the value of the satellite data for limnological studies which depend so heavily on temporal comparisons. The systematic overflight program would have significant impact on the cost of eutrophication monitoring for large lakes and systems of large lakes.

ACKNOWLEDGMENT

The authors wish to acknowledge the enthusiastic cooperation and assistance of Mr. Larry B. York of the Principal Investigations Management Office at the Johnson Space Center, who was the Technical Monitor of the contract.

Section 6

REFERENCES

1. Optical Properties of Lake Ontario Waters, National Science Foundation Grant No. GA-37768.

2. A. Beeton, "Relationship Between Secchi Disk Readings and Light Penetration in Lake Huron," Trans. Am. Fish. Soc., Vol. 87, 1968, pp. 73-79.

3. J. Graham, "Secchi Disk Observations and Extinction Coefficients in the Central and Eastern North Pacific Ocean," Limnol. Oceanogr., Vol. 11, 1966, pp. 184-190.

4. E.G. Fruh, K.M. Stewart, G.F. Lee, and G.A. Rohlich, "Measurements of Eutrophication Trends," J. Wat. Pollut. Control Fed., Vol. 38, 1966, pp. 1237-1258.

5. K.M. Stewart and G.A. Rohlich, "Eutrophication - A Review," Calif. St. Wat. Qual. Control Bd., Publ. No. 34, 1967, 188 p.

6. G.E. Likens (ed.), "Nutrients and Eutrophication: The Limiting Nutrient Controversy," Special Symposia, Vol. I, Limnol. Oceanogr., 1972, 328 p.

7. H.F.H. Dobson, M. Gilbertson, and P.G. Sly, "A Summary and Comparison of Nutrients and Related Water Quality in Lakes Erie, Ontario, Huron, and Superior," J. Fish. Res. Board Can., Vol. 31, 1974, pp. 731-738.

8. K. R. Piech, "International Field Year on the Great Lakes: Optical Properties of Lake Ontario Waters", Calspan Corporation Report No. KS-5108-M-1, November 1972.

9. K. R. Piech and J. E. Walker, "Aerial Color Analyses of Water Quality", Journal of the Surveying and Mapping Division, ASCE, Vol. 97, No. SU2, November 1971, pp. 185-197.

10. K. R. Piech and J. E. Walker, "Thematic Mapping of Flooded Acreage", Photogrammetric Engineering, Vol. 38, November 1972, pp. 1081-1090.

11. K. R. Piech and J. E. Walker, "Interpretation of Soils", Photogrammetric Engineering, Vol. 40, January 1974, pp. 87-94.

12. P. G. Smith, K. R. Piech and J. E. Walker, "Special Color Analysis Techniques", Photogrammetric Engineering, Vol. 40, November 1974, pp. 1315-1322.

13. K.R. Piech and J.R. Schott, "Atmospheric Corrections for Satellite Water Quality Studies," Proceedings of the SPIE, Volume 51, August 1974, pp. 84-89.

14. "ERTS Image Processing System Performance Prediction and Product Quality Evaluation Techniques", NASA Contract NAS5-20366.

Section 7

LIST OF KEY SYMBOLS

α	Exposure parameter proportional to atmospheric transmittance and total irradiance (sunlight + skylight)
α'	Exposure parameter proportional to atmospheric transmittance and skylight irradiance
β	Flare exposure caused by atmospheric and camera flare
D	Film density
E	Film exposure of an object in sunlight
E'	Film exposure of an object in shadow
λ, λ_i	Subscripts denoting a specific spectral band
R	Object reflectance
R_V	Volume relfectance of a body of water
R_S	Surface or Fresnel reflectance of a body of water
r	Diffuse reflectance of a slab
r_2	Diffuse reflectance of a slab of double thickness
S	Total signal received by a sensor
s	Signal received by a sensor which is solely due to the water medium
σ	Standard deviation
t	Total transmission through a slab
t_2	Total transmission through a slab of double thickness
$\bar{x}$	Mean